Philosophical Magazine A

ISSN: 0141-8610 (Print) 1460-6992 (Online) Journal homepage: https://www.tandfonline.com/loi/tpha20

The atomic structure of a [100], 45° twist plus 17.5° tilt grain boundary in aluminium by high-resolution electron microscopy

M. Shamsuzzoha , D. J. Smith & P. A. Deymier

To cite this article: M. Shamsuzzoha , D. J. Smith & P. A. Deymier (1991) The atomic structure of a [100], 45° twist plus 17.5° tilt grain boundary in aluminium by high-resolution electron microscopy, Philosophical Magazine A, 64:3, 719-733, DOI: 10.1080/01418619108204870

To link to this article: https://doi.org/10.1080/01418619108204870

PHILOSOPHICAL MAGAZINE A, 1991, VOL. 64, NO. 3, 719–733

The atomic structure of a [100], 45° twist plus 17·5° tilt grain boundary in aluminium by high-resolution electron microscopy

By M. SHAMSUZZOHA†, DAVID J. SMITH‡ and P. A. DEYMIER†

† Department of Materials Science and Engineering, University of Arizona, Tucson, Arizona 85721, USA
‡ Center for Solid State Science and Department of Physics, Arizona State University, Tempe, Arizona 85287, USA

[*Received 19 July 1990 and accepted 5 November 1990*]

ABSTRACT

A [100], 45° twist plus 17·5° tilt mixed character aperiodic grain boundary in aluminium has been studied by high-resolution electron microscopy. Most of the boundary is asymmetric and exhibits coherency and/or anticoherency dislocations due to lattice mismatch across the interface. The boundary structure was found to be constituted of two basic structural units and could not be characterized on the basis of coincident-site lattice, displacement shift complete and the O-lattice geometric models of grain boundaries. Steps and microfacets observed at the boundary have also been characterized within the framework of the same structural unit model.

§ 1. INTRODUCTION

Grain-boundary structures have been the subject of many theoretical and experimental investigations, ever since it was realized that they play a key role in determining many physical properties in polycrystalline materials. The structure of grain boundaries can be described in terms of geometrical models based on coincident-site lattice (CSL) (Kronberg and Wilson 1964, Smith and Pond 1976) displacement shift complete (DSC) lattice (Smith and Pond 1976, Bollman 1970, Balluffi 1977) and the O-lattice theories (Bollman 1970). However, despite their usefulness in characterizing the global nature of the grain-boundary structure, these models still prove to be inadequate in providing a thorough understanding of atomic relaxations that may occur at the grain-boundary core. Furthermore, these models are only applicable to periodic grain boundaries. Further advances in elucidating the relaxation processes that occur at the grain-boundary core have been achieved with the development of simulations for the structure of periodic grain boundaries using atomistic modelling by molecular statics and molecular dynamics (Vitek, Sutton, Smith and Pond 1980).

One significant aspect which emerges from the continued efforts to improve our knowledge of the structure of grain boundaries is the presence of some recurring structural unit in periodic grain boundaries. The structural unit principle in grain boundaries was originally put forward by Sutton and Vitek (1983) based on studies of the simulated structure of a large number of periodic grain boundaries in aluminium and copper. These workers proposed the existence of some low-energy ordered boundaries (called 'favoured' boundaries), with cores constituted from the basic structural unit. Other boundaries that deviated from these specific orientations in an attempt to minimize the overall energy of the boundary may assume a core structure composed of one or more of these basic structural units. This model which involves a

structural unit (Bristowe and Balluffi 1985) is equivalent to the secondary grain-boundary dislocation (SGBD) model in which a SGBD forms to accommodate the deviation from an 'ordered interface'. High-resolution electron microscopy (HREM) has now provided experimental evidence for the structural unit model. Symmetrical ⟨110⟩ tilt boundaries of gold with misorientations ranging between 0 and 109° have shown the existence of at least three low-energy basic structural units (Ichinose and Ishida 1981, 1985, Krakow, Wetzel and Smith 1986).

In spite of these advances, the structure of aperiodic grain boundaries has not been characterized systematically with any success either by the existing geometrical models of grain boundaries or by computer simulation. In this paper we present an example of such an aperiodic grain boundary, with a structure that cannot be described within the framework of CSL, DSC lattice and the O-lattice theories. Analyses of high-resolution images revealed that the boundary exhibits some well defined structural units that are arranged systematically along the entire length of the boundary.

§2. Experimental procedures

The aluminium bicrystal used for this study was prepared by cold rolling and annealing using a method described in detail elsewhere (Shamsuzzoha and Deymier 1990). For thin-foil preparation, cylindrical specimens of 3 mm diameter containing the boundary were trepanned by spark cutting. The cylindrical discs were polished gently on 600 grade silicon carbide paper to reduce their thickness to 0·3 mm or less. Finally, the discs were electropolished in a solution consisting of 250 mm^3 of nitric acid, 250 mm^3 of methanol and 20 mm^3 of hydrochloric acid at a voltage of 50 V at room temperature.

The thin foils thus prepared were examined with a 120 kV Hitachi electron microscope, and angle–axis orientation relationships of the mixed-character boundaries were determined. HREM was performed with a JEM-4000EX operated at 400 kV. High-resolution electron micrographs were recorded near the optimum defocus typically at a magnification of 500 000 times. The atomic columns appear black under these experimental conditions so that the atomic structure in the vicinity of the grain boundary was resolved unambiguously.

§3. Grain-boundary morphology

A high-resolution electron micrograph of a mixed-character boundary in aluminium, taken with the electron beam parallel to [001] of crystal 1 and [011] of crystal 2, is shown in fig. 1. The mixed character of the boundary can be described in terms of a [100], 45° twist rotation followed by a 17·5° tilt rotation about the common $[001]_1$ and $[011]_2$. Most of the boundary is asymmetric, and parallel to the (010) plane of crystal 1 and approximately the $(49\bar{9})$ plane of crystal 2.

§4. Theoretical discussion

4.1. *Dichromatic patterns and geometrical models*

The structural characterization of this mixed-character boundary requires a prior discussion of the geometrical model for a perfect [100], 45° twist boundary, which then allows a better understanding of the complex structure which follows from a subsequent introduction of additional tilt character into the twist boundary.

The dichromatic patterns of the [100] twist boundary of a f.c.c. crystal, as viewed along the [100] twist axis as well as along the common $[001]_1$ or $[011]_2$ direction normal to the twist axis, are given in figs. 2(*a*) and (*b*). The patterns exhibit an 8′/m mm′ group symmetry [13], where 8′ represents an eightfold rotation axis relating atoms of the two interpenetrating crystals, m and m′ represent mirror planes between atoms of the same crystal and coloured mirror planes between atoms of the interpenetrating crystals respectively. In the $[001]_1$ or $[011]_2$ projection, the dichromatic patterns exhibit continuity of the $(100)_1$ and $(100)_2$ crystal planes.

The 8′/m mm′ symmetry of the dichromatic patterns is incompatible with periodicity. Therefore the Σ value of the CSL for a [100], 45° twist boundary assumes an infinite value, and the DSC lattice vectors for this dichromatic pattern become infinitely small. By taking into consideration the 0·3° experimental uncertainty on the twist misorientation of the investigated grain boundary, the closest CSL is $\Sigma = 169$ ($\theta = 44{\cdot}790°$), which has a very large CSL unit cell and correspondingly very small DSC lattice vectors. The assignment of the CSL and DSC unit cell for very large to infinite Σ becomes unnecessary, and thus the boundary characterization on the basis of the CSL and DSC lattice geometrical models is meaningless. However, some O-lattice type directions, which pass through points of best match between lattices of interpenetrating crystals, present within the dichromatic patterns can be easily visualized. From the viewpoint of the bicrystal group symmetry, the O-lattice direction (or direction of best match) is either parallel or perpendicular to mirror planes relating atoms of two interpenetrating crystals (or coloured mirror planes). These directions derived from O-lattice theory, referred to the lattice of crystal 1 (represented by full circles in figs. 2(*a*) and (*b*)), are given by

$$X_1^{(0)} = \begin{vmatrix} 0 \\ \left(2 - \dfrac{3}{2^{1/2}}\right) \\ \left(1 - \dfrac{1}{2^{1/2}}\right) \end{vmatrix},$$

$$X_2^{(0)} = \begin{vmatrix} 0 \\ \left(\dfrac{1}{2^{1/2}} - 1\right) \\ \left(2 - \dfrac{3}{2^{1/2}}\right) \end{vmatrix},$$

$$X_3^{(0)} = \begin{vmatrix} 2 - 2^{1/2} \\ 0 \\ 0 \end{vmatrix}.$$

Upon insertion of additional tilt about the common $[001]_1$ and $[011]_2$ by some arbitrary amount θ to the [100], 45° twist boundary, the one-to-one correspondence between the $(100)_1$ and $(100)_2$ planes is lost. The dichromatic patterns of such a misorientation described by a [100], 45° twist plus 17·5° tilt as viewed along $[001]_1$ and $[011]_2$ directions are shown in fig. 3(*a*). Additional tilt in the dichromatic pattern results in a decrease in the dichromatic pattern group symmetry from 8′/m mm′ at the

[100], 45° twist boundary to m′m′m. The transformation matrix describing a 45° twist plus $\theta = 17{\cdot}5°$ tilt misorientation is given by

$$[A] = \frac{1}{2^{1/2}} \begin{vmatrix} 1{\cdot}0000 & -1{\cdot}0000 & 0{\cdot}0000 \\ 0{\cdot}9560 & 0{\cdot}9560 & 0{\cdot}2924 \\ -0{\cdot}2924 & -0{\cdot}2924 & 0{\cdot}9550 \end{vmatrix}.$$

Fig. 1

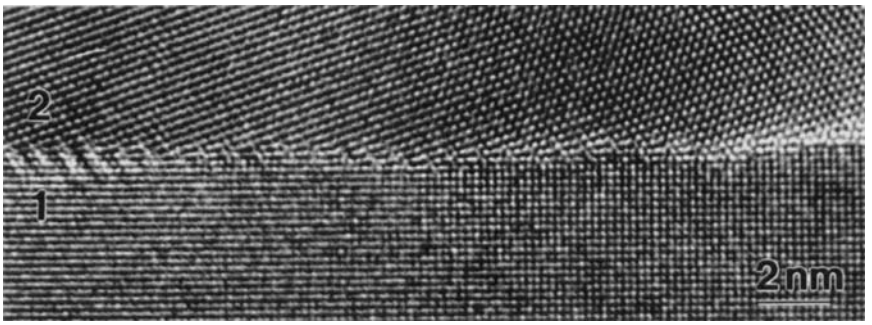

High-resolution electron micrograph showing the [100], 45° twist plus 17·5° tilt grain boundary in aluminium. The incident electron beam is parallel to $[001]_1$ and $[011]_2$.

Fig. 2

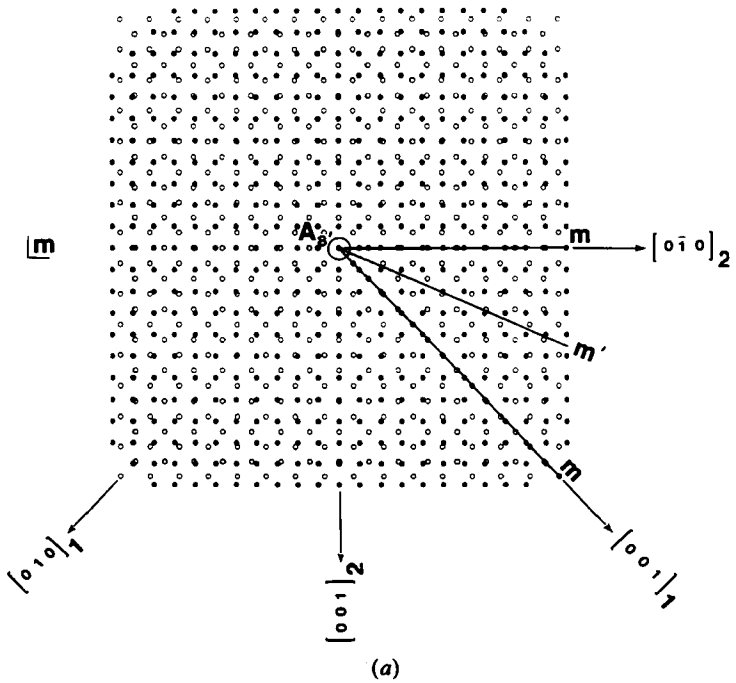

(*a*)

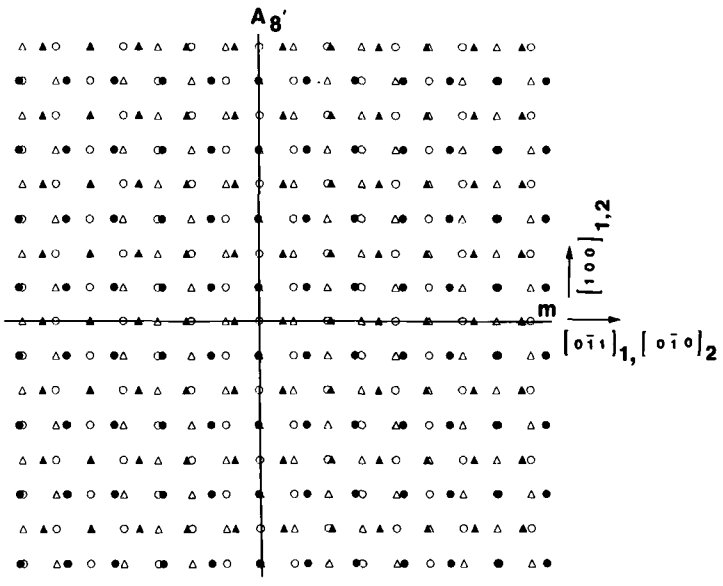

(*b*)

(*a*) Dichromatic patterns of the [100], 45° twist grain boundary as viewed along the twist axis $[100]_{1,2}$. Crystals 1 and 2 are represented by full and open circles respectively. (*b*) As for (*a*) but viewed along $[001]_1$ or $[011]_2$. Open and full circles and triangles represent two successive atomic stacking along $[001]_1$ and $[011]_2$ planes respectively.

This misorientation does not produce any coincidence site, but at the origin. Furthermore, an extensive search for the CSL at a misorientation of 44·76° twist plus 13–20° tilt, caused the CSLs to have very large Σ values. Of particular interest, the coincidence site found at a tilt angle of 17·491° has a Σ value greater than 1000. Hence, characterization of the observed grain boundary on the basis of atomic coincidence seems impracticable. On the other hand, the O-lattice directions which run parallel to m′ (colour mirror plane) symmetry lines of the dichromatic patterns can be expressed in the framework of crystal 1 (represented by full circles in fig. 3(*a*)) as

$$X_{1'}^{(0)} = \begin{vmatrix} -2^{1/2} \\ 1 \\ 0 \end{vmatrix},$$

$$X_{2'}^{(0)} = \begin{vmatrix} 2-2^{1/2} \\ -1 \\ 0 \end{vmatrix},$$

$$X_{3'}^{(0)} = \begin{vmatrix} -1 \\ -1 \\ (1-2^{1/2}) \end{vmatrix}.$$

Fig. 3

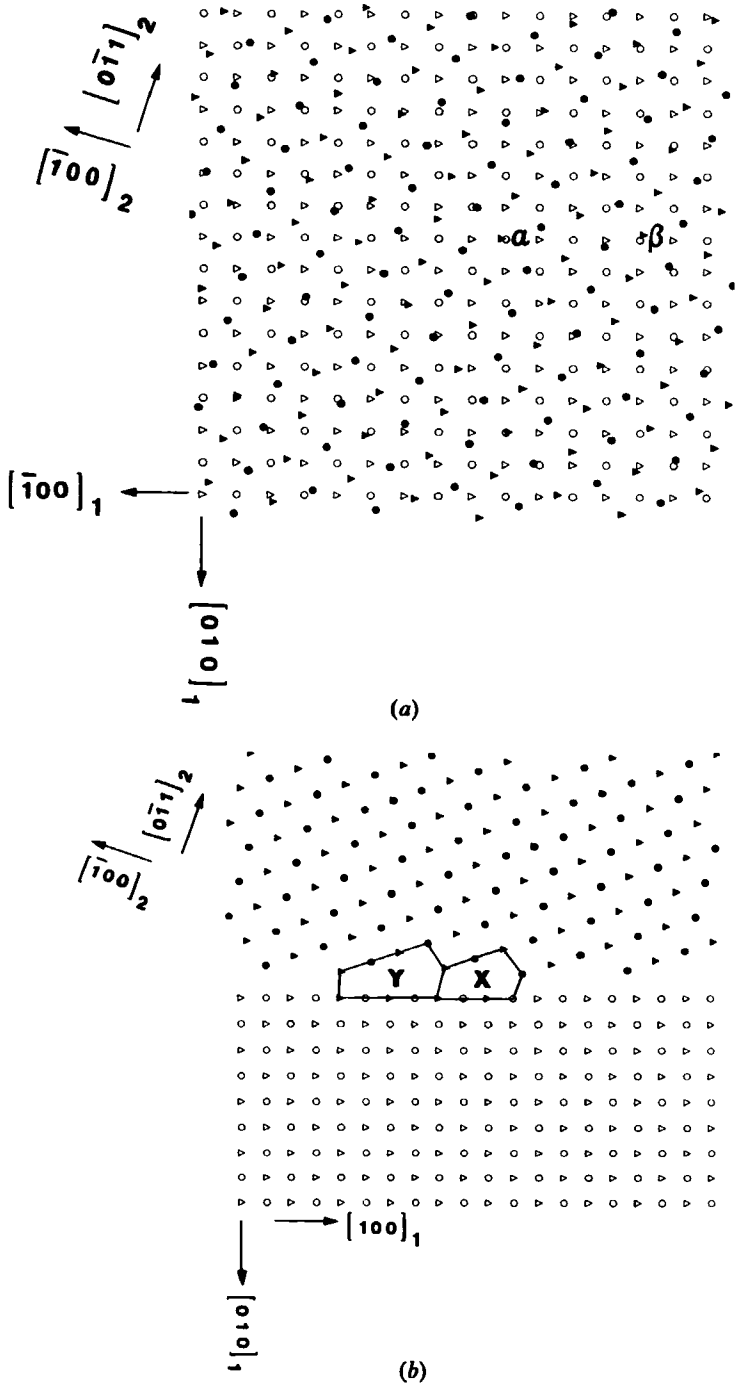

(*a*) Dichromatic patterns of the [100], 45° twist plus 17·5° tilt grain boundary as viewed along the $[001]_1$ or $[011]_2$ direction normal to twist axis. The symbols are the same as in fig. 2(*b*). (*b*) A [100], 45° twist plus 17·5° tilt bicrystal, showing basic structural units labelled X and Y. The symbols are the same as in fig. 2(*b*).

Interestingly, the observed grain-boundary plane inclination along $(010)_1$ and $(49\bar{9})_2$ is not parallel to these directions of best match, implying that this particular direction does not provide any insight into the nature of the grain boundary. Therefore some criterion other than the lattice match must be used to describe the grain-boundary structure.

4.2. *Structural unit model*

Because of the inadequacy of the CSL, DSC lattice and the O-lattice models for describing the mixed-character boundary, it seems desirable to introduce the concept of structural unit models to characterize the boundary. A rigid two-dimensional bicrystal can be constructed from the dichromatic patterns illustrated in fig. 3 (*a*) by introducing a plane parallel to $(010)_1$ and $(49\bar{9})_2$ and disregarding the atoms labelled by open circles and triangles from one side of the plane and the atoms labelled by full circles and triangles from the other side. Figure 3 (*b*) shows the $[001]_1$ or $[011]_2$ view of the bicrystal. Crystal 1 is periodic along the $[010]_1$ direction with a period of a (a being the lattice parameter). Crystal 2 is also periodic along the $[49\bar{9}]_2$ direction with a period of 3·764 nm. Thus within this bicrystal there is no one-to-one lattice match along the boundary. However, owing to a ratio of periods along the boundary plane equal to about 9·4, one may be able to interpret the lattice matching at the interface in terms of a 'pseudo-coincidence'. For example, the lattice points labelled α and β in the dichromatic patterns in fig. 3 (*a*) can be thought of as being almost coincident.

By inspection, it can be found that for tilt values $\theta = 13{\cdot}29°$ and 19·47° with respect to the grain-boundary plane location along $(010)_1$, a similar 'pseudo-coincidence' occurs after every approximately three and four spacings respectively in reference to crystal 1. These tilt angles correspond to the $(13\bar{3})_2$ and $(12\bar{2})_2$ grain-boundary plane inclinations. In the corresponding bicrystals (figs. 4 (*a*) and (*b*)), the atoms contained between any two adjacent 'pseudo-coincidences' of interface lattices are arranged in a well defined structural unit in the immediate neighbourhood of the interface. The structural units (as outlined in fig. 4) are correspondingly labelled as X and Y units. Within each structural unit, atoms belonging to the neighbouring grains lie on their respective $(010)_1$ and $(1\bar{1}1)_2$ planes. In this configuration, the most closely spaced atomic pair at the interface is thought to be attached by some form of 'bridging bond'. Owing to their relatively large separation across the interface, other atoms of the structural units remain influenced by the bonding of the matrix crystal.

The structural units so far described are purely two dimensional. For a three-dimensional description, the lattice arrangement along the depth of the bicrystals needs to be considered. Figure 5 (*a*) shows the interface lattice arrangement in projection for all bicrystals. It exhibits a $(001)_1$ and $(011)_2$ lattice arrangement. Because of the irrational value of $2^{1/2}$ for the ratio of $(001)_1$ and $(011)_2$ plane spacings, these lattices cannot coincide on a one-to-one basis at the interface, although a 'pseudo-coincidence' occurs every other 14 $(001)_1$ or 20 $(011)_2$ interplanar spacings. By considering this 14 $(001)_1$ or 20 $(011)_2$ 'pseudo-coincidence' along the depth of the interface, a three-dimensional grain-boundary structural unit is constructed and is shown in fig. 5 (*b*).

Considering that coherency across the interface may be associated with low interfacial energy, a similar mixed-character boundary with a tilt angle of 17·5° is expected to be constituted of a mixture of X and Y structural units. Because of its closeness to the 19·47° tilt mixed-character boundary, this boundary is expected to exhibit a greater frequency of occurrence for the structural unit Y relative to the unit X. The 17·5° tilt boundary may be constructed by a sequence of X and Y units in the ratio of 1 to 4.

Fig. 4

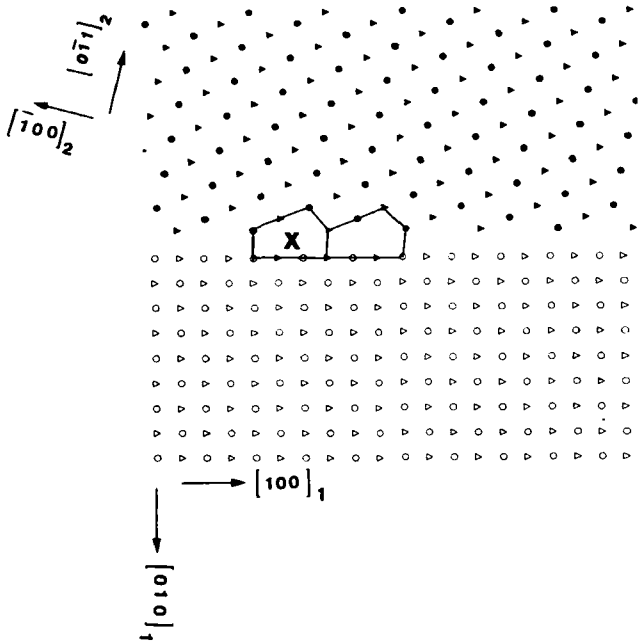

(*a*)

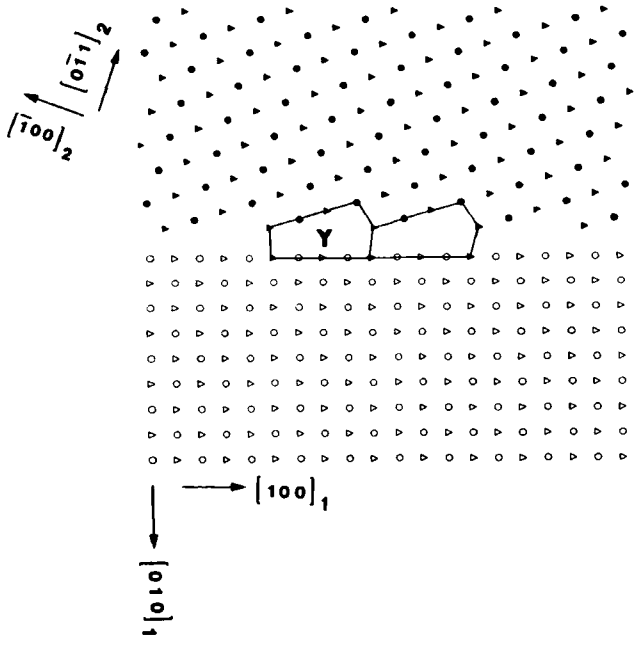

(*b*)

(*a*) Bicrystal of the [100], 45° twist plus 13·27° tilt grain boundary as viewed along the $[001]_1$ or $[011]_2$ direction exhibiting the grain-boundary structural unit X. The symbols are the same as in fig. 2 (*b*). (*b*) A [100], 45° twist plus 19·47° tilt bicrystal as viewed along [001] or $[011]_2$ direction, exhibiting the grain-boundary structural unit Y.

Fig. 5

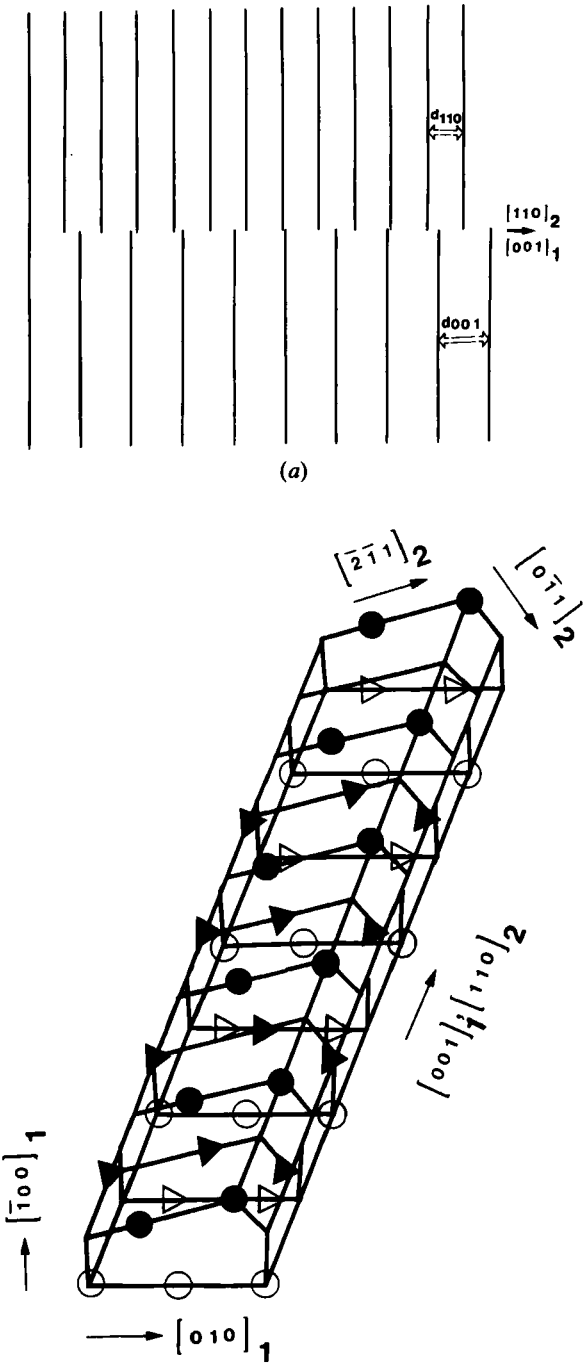

(*a*) Interface lattice arrangement of the [100], 45° twist plus arbitrary θ° tilt bicrystal as viewed along the $[001]_1$ or $[110]_2$ direction. (*b*) Schematic diagram showing the three-dimensional configuration of structural unit Y.

4.3. *Misfit or anticoherency dislocations*

As discussed earlier, a mixed-character boundary with any arbitrary tilt angle θ does not exhibit lattice coincidence across the interface. For instance, in a $\theta = 19{\cdot}47°$ mixed-character boundary (fig. 4(*b*)), the $(100)_1$ and $(001)_1$ planes do not exhibit a one-to-one lattice correspondence with $(100)_2$ and $(011)_2$ planes respectively. The resulting lattice misfit at the interface can be seen to be replaced by a progressive bending of the 'bridging bond' of the structural unit in both the $[49\bar{9}]_2$ and the $[011]_2$ directions. This process of bending of the 'bridging bond' continues until a misfit or anticoherency dislocation forms at the interface to reestablish the initial alignment of the 'bridging bond'.

§ 5. Experimental results and discussion

5.1. *Grain-bondary structure*

A visual inspection of the experimental boundary (fig. 1) immediately identifies the crystalline nature of the interface. The high-magnification view (fig. 6(*a*)) of a typical boundary segment reveals the existence of a well defined atomic arrangement. In accordance with the theoretical discussion above on the structural unit model of the boundary, the experimental image gives a structure (fig. 6(*b*)) which is indeed constituted of the structural units X and Y. In other words, these X and Y structural units are arranged systematically along the boundary plane roughly in the ratio of 1 to 4. The structural units present in the experimental boundary, upon comparison with their rigid-body counterparts in fig. 4, exhibit slight distortion in their geometrical shape. This clearly implies that the grain-boundary core has undergone some relaxation.

The relaxation process can be understood from the fact that atoms in a distorted region of space such as a grain boundary tend to achieve the least energetic interatomic spacing. For a f.c.c. crystal the most stable interatomic spacing is $a/2^{1/2}$, when a is the lattice parameter. Figure 7 illustrates the speculated atomic relaxation within the grain boundary. The atoms labelled P_1 and P_2 forming what is called a 'bridging bond' coexist in the low-energy atomic spacing of $a/2^{1/2}$. However, the angle between neighbouring $(010)_1$ and $(1\bar{1}1)_2$ planes across the interface forces the neighbouring atoms Q_1 and Q_2 of the structural unit, to be located further away than the stable spacing by about 20%. Therefore it is anticipated that this pair of atoms will relax to assume a more stable interatomic spacing simply by displacing the atom Q_1 towards the atom Q_2. On the other hand, the atom R_1 in fig. 7 is so far away from the atom R_2 that it remains trapped within the bonding influence of the matrix of crystal 2 and may not take part in the relaxation process.

The resulting strain due to the grain-boundary core relaxation is likely to affect the resolution of the HREM images of the boundary. The strain contrast observed in the HREM image of fig. 6(*a*) shows such an influence. Moreover, as expected, the periodicity of the strain contrast present in the HREM image follows the periodicity of the structural unit at the boundary plane.

Careful inspection of the high resolution image of fig. 6(*a*) also reveals the presence of misfit or anticoherency dislocations (Olson and Cohen 1979). Such a dislocation is located at the position marked as D in fig. 6(*b*). A closed circuit projected on the plane of the micrograph has been drawn around a defect-free portion of the grain boundary for reference. An identical circuit enclosing the defective segment of the grain boundary gives a closure failure vector of about $\frac{1}{2}[100]$. However, in the absence of any three-dimensional structural analysis of the boundary, it seems undesirable to consider this

Fig. 6

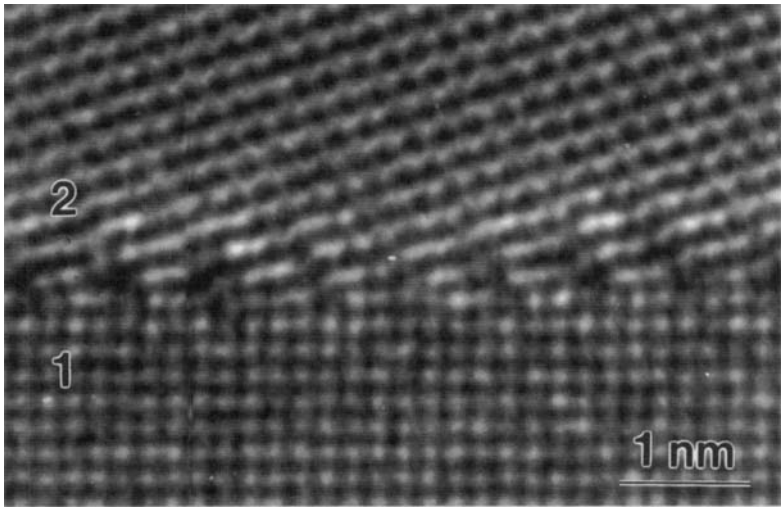

(*a*)

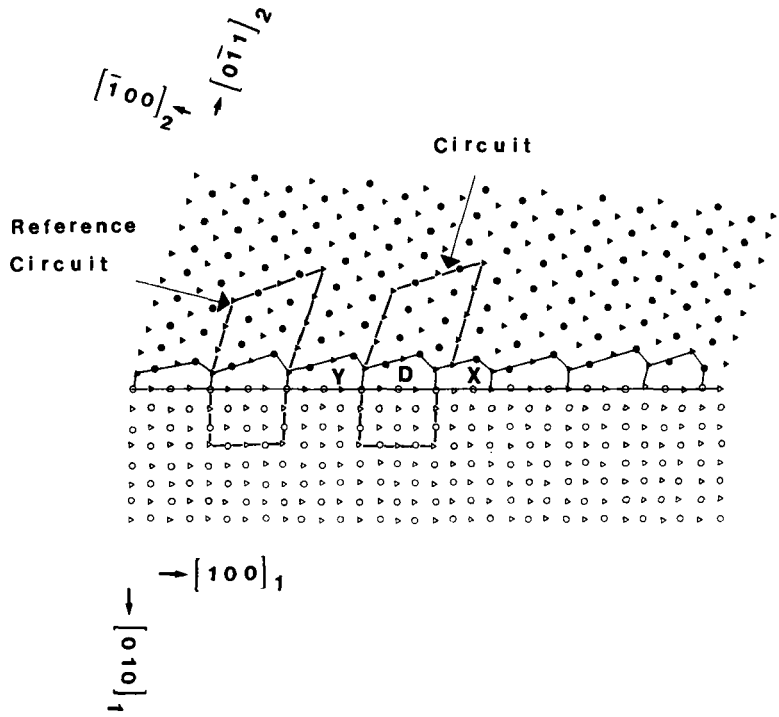

(*b*)

(*a*) High-magnification view taken from the [100], 45° twist plus 17·5° tilt boundary shown in fig. 1. (*b*) Possible projected atomic positions in (*a*). Dislocation circuits are drawn around the misfit dislocation indicated as D.

Fig. 7

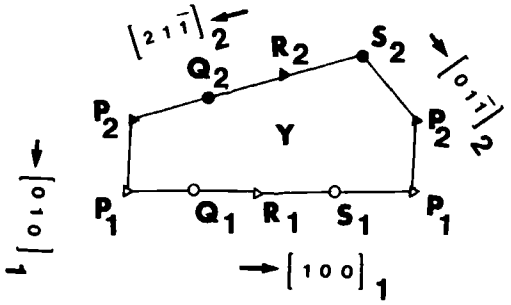

Schematic representation of atomic relaxation in a 19·47° structural unit Y (see text for explanation).

closure failure vector as the actual Burgers vector for the dislocation. The closure failure certainly indicates the presence of an extra half-plane, indicating the existence of a misfit or anticoherency dislocation at the boundary. In a two-dimensional representation, the structural units on either side of the anticoherency dislocation appear to possess a different atomic configuration. However, a careful inspection of the three-dimensional structural unit shown in fig. 5 (*b*) indicates that the structural unit observed at the general boundary as well as that present near the anticoherency dislocation corresponds approximately to two non-equivalent planes along the tilt axis of the same three-dimensional unit. Thus the structure is conserved across the coherency dislocation.

5.2. *Grain-boundary stepping and facets*

Stepping in periodic boundaries is generally associated with secondary grain-boundary dislocations in order to conserve the grain-boundary structure; so it is of interest to see how grain-boundary stepping occurs in an aperiodic grain boundary. Efforts were made to look for such stepping in the experimental boundary. A $\frac{1}{2}$[010] step is shown at the position marked B in fig. 8 (*a*). A circuit identical with the closed reference circuit defined in fig. 6 (*a*) drawn around this step gives a closure failure vector of magnitude less than $\frac{1}{2}$[100]. This closure failure cannot be related to any secondary dislocation since the DSC lattice is impracticably small for the particular bicrystal. It is, however, noteworthy that this closure failure is similar to that observed for coherency dislocations (Olson and Cohen 1979).

The grain-boundary stepping also allows the structural unit to shift by one layer along the [010] direction. The two-dimensional structural units across the step (fig. 8 (*a*)) exhibit a change in 'bridging bond' identical with that observed at the interface containing anticoherency dislocations. Thus the corresponding three-dimensional structural unit is again conserved at the step. Upward and downward stepping occurs regularly along the grain boundary (fig. 9). It appears that stepping may offer a mechanism of conservation of the grain-boundary core structure in terms of the basic structural units.

In addition to steps, the boundary also exhibits microfaceting. One such facet present at the boundary is shown in fig. 10 (*a*). It exhibits a visual symmetry across the interface and is parallel to $(\bar{5}10)$ of crystal 1 and $(5\bar{8}5)$ of crystal 2, neither of which lies along the O-lattice direction. Along the entire length of the facet, a reasonable distorted

Fig. 8

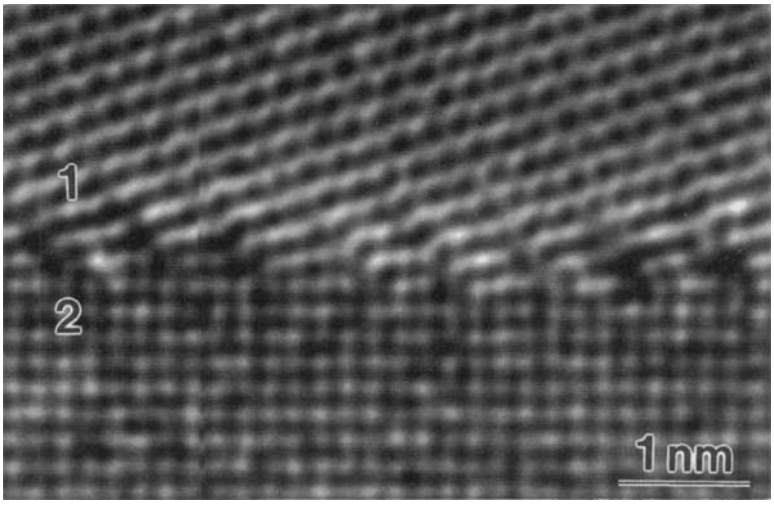

(*a*)

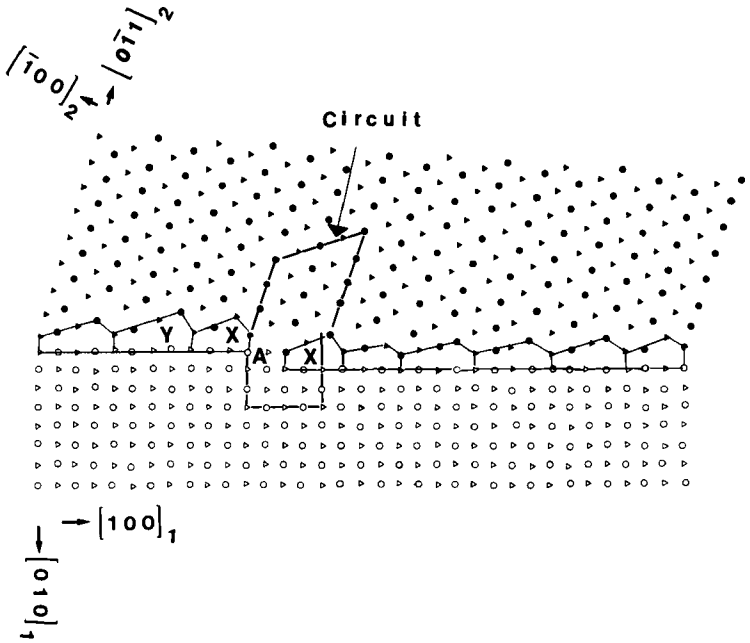

(*b*)

(*a*) High-magnification view of side step taken from the [100], 45° twist plus 17·5° tilt boundary shown in fig. 1. (*b*) Possible projected atomic positions in (*a*). The dislocation circuit is drawn around the step indicated as A.

Fig. 9

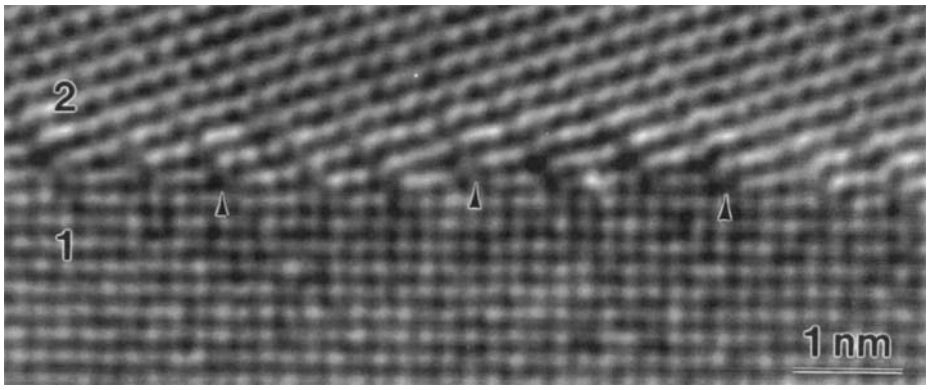

HREM micrograph showing alternating grain-boundary stepping at positions marked by arrow in the [100], 45° plus 17·5° tilt grain boundary.

Fig. 10

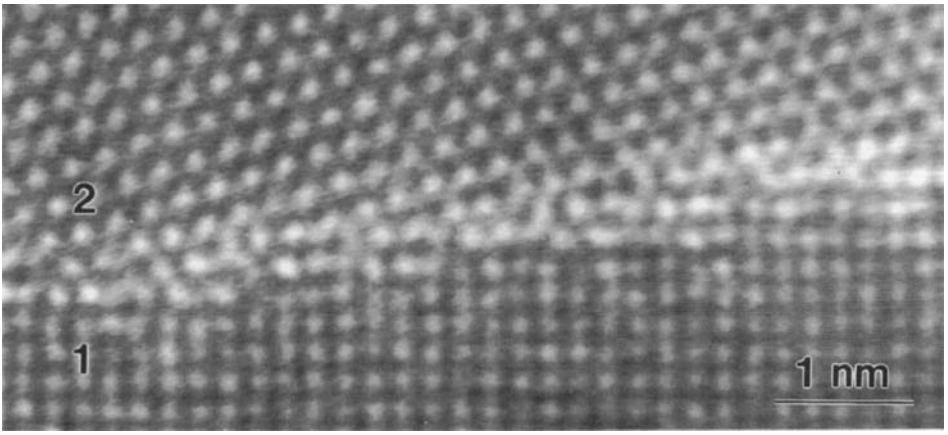

(*a*)

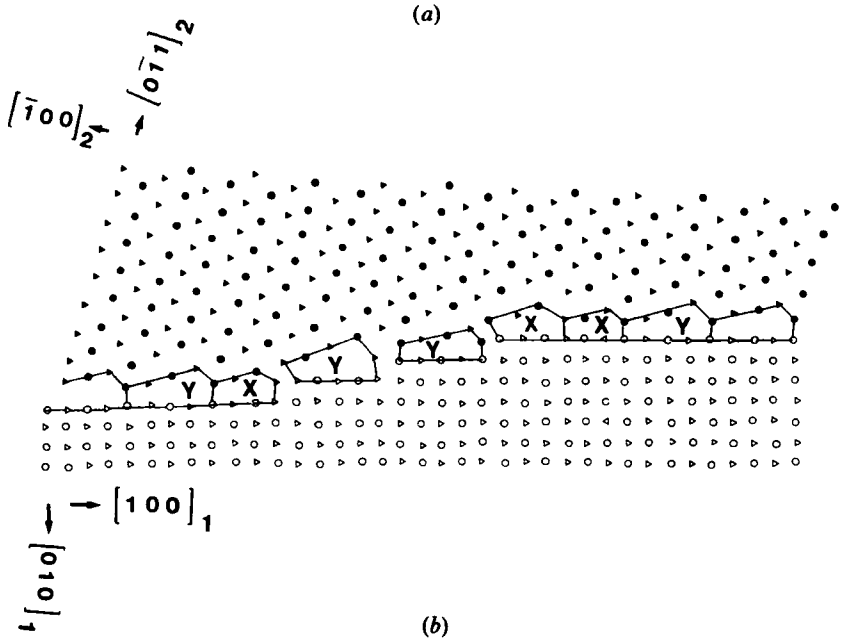

(*b*)

(*a*) HREM micrograph of the [100], 45° twist plus 17·5° tilt grain boundary exhibiting microfaceting along $(\bar{5}10)_1$ or $(5\bar{8}5)_2$. (*b*) Possible projected atomic positions in (*a*).

version of the X and Y structural unit is arranged in a succession of $\frac{1}{2}[010]$ steps (fig. 10(*b*)). Although the high-resolution image of the facet seems to contain a lesser degree of strain contrast, the physical reason for this is unclear and further studies are in progress.

§6. Conclusions

From this investigation, the following conclusions can be drawn.

(1) Theoretical concepts can be developed for the application of structural unit models in aperiodic [100], 45° twist plus tilt grain boundaries.
(2) Evidence has been presented for the validity of the structural unit model in an aperiodic grain boundary in aluminium, as described by a [100], 45° twist followed by a 17·5° tilt about the common $[001]_1$ or $[011]_2$ direction normal to the twist boundary. The structure along the length of its asymmetric boundary (e.g. $(010)_1$ or $(49\bar{9})_2$), constituted of a mixture of two basic structural units, where each unit constitutes the sole structure of similar boundaries formed at tilt angles $\theta = 13{\cdot}29°$ and 19·47°.
(3) The conservation of the structural unit character at the grain boundary results in the development of coherency and/or anticoherency dislocations along the grain-boundary plane.
(4) The structural unit character of the grain boundary is also conserved at the grain-boundary steps and facets.

Acknowledgments

This research utilized the Facility for High Resolution Electron Microscopy in the Center for Solid State Science at Arizona State University, established with support from the National Science Foundation (Grant No. DMR-86-11609). The authors also acknowledge the receipt of financial support from the U.S. Department of Energy under Contract No. DE-FG02-87ER45285.

References

Balluffi, R. W., 1977, *Interfacial Segregation*, edited by W. C. Johnson and J. M. Blakely (Metals Park, Ohio: American Society for Metals).
Bollmann, W., 1970, *Crystal Defects and Crystalline Interfaces* (New York: Springer), p. 193.
Bristowe, P. D., and Balluffi, R. W., 1985, *J. Phys., Paris*, **46**, C4–155.
Ichinose, H., and Ishida, Y., 1981, *Phil. Mag.*, **43**, 1253; 1985, *J. Phys., Paris*, **46**, C4–39.
Krakow, W., Wetzel, J. T., and Smith, D. A., 1986, *Phil. Mag.* A, **53**, 739.
Kronberg, M. L., and Wilson, F. M., 1964, *Am. Inst. Min. metall. Petrol Engrs*, **85**, 26.
Olson, G. B., and Cohen, M., 1979, *Acta metall.*, **22**, 1907.
Shamsuzzoha, M., and Deymier, P. A., 1990, *Scripta metall. Mater.*, **24**, 1303.
Smith, D. A., and Pond, R. C., 1976, *Int. Metals Rev.*, **205**, 61.
Sutton, A. P., and Vitek, V., 1983, *Phil. Trans. R. Soc.* A, **309**, 1.
Vitek, V., Sutton, A. P., Smith, D. A., and Pond, R. C., 1980, *Grain Boundary Structure and Kinetics*, edited by R. W. Balluffi (Metals Park, Ohio: American Society for Metals), p. 115.